

24. McFarland, K. C. *et al. Science* **245**, 494–499 (1989).
 25. Shapiro, R. A., Schrer, N. M., Habecker, B. A., Subers, E. M. & Nathanson, N. M. *J. Biol. Chem.* **263**, 18397–18403 (1988).
 26. Chee, M. S., Satchwell, S. C., Preddie, E., Weston, K. M. & Barrell, B. G. *Nature* **344**, 774–777 (1990).

ACKNOWLEDGEMENTS. We thank S. Nakanishi (Kyoto University), and K. Takahashi, K. Inoue and I. Kudo (University of Tokyo) for suggestions, and M. Ohara for comments. This work was supported in part by grants from the Ministry of Education, Science and Culture; the Ministry of Health and Welfare of Japan; and the Mitsubishi Foundation.

Control of the sperm–oocyte switch in *Caenorhabditis elegans* hermaphrodites by the *fem-3* 3' untranslated region

Julie Ahringer & Judith Kimble*

Department of Biochemistry, College of Agricultural and Life Sciences, and Laboratory of Molecular Biology, Graduate School, University of Wisconsin-Madison, Madison, Wisconsin 53706, USA

IN the *Caenorhabditis elegans* hermaphrodite germ line, sperm and then oocytes are made from a common pool of germ-cell precursors. The decision to differentiate as a sperm or an oocyte is regulated by the sex-determining gene, *fem-3*. Expression of *fem-3* in the hermaphrodite germ line directs spermatogenesis and must be negatively regulated to allow the switch to oogenesis^{1,2}. In adult hermaphrodites (which are producing oocytes), most *fem-3* RNA is found in the germ line³, consistent with both the requirement for *fem-3* in hermaphrodite spermatogenesis and the maternal effects of *fem-3* on embryonic sex determination^{1,2}. Whereas loss-of-function mutants in *fem-3* produce only oocytes, hermaphrodites carrying any of nine *fem-3* gain-of-function (*gf*) mutations make none; instead sperm are produced continuously and in vast excess over wild-type amounts¹. Genetic analyses suggest that *fem-3(gf)* mutations have escaped a negative control required for the switch to oogenesis¹. Here we report that all nine *fem-3(gf)* mutants carry sequence alterations in the *fem-3* 3' untranslated region (3' UTR). There is no increase in the steady-state level of *fem-3(gf)* RNA over wild-type, but there is an increase in the polyadenylation of *fem-3(gf)* RNA that is coincident with the unregulated *fem-3* activity. Results of a titration experiment support the hypothesis that a regulatory factor may bind the *fem-3* 3' UTR. We speculate that *fem-3* RNA is regulated through its 3' UTR by binding a factor that inhibits translation, and discuss the idea that this control may be part of a more general regulation of maternal RNAs.

To learn how *fem-3(gf)* mutations affect the regulation of *fem-3*, we sequenced two *fem-3(gf)* alleles, *q20* and *q22*, in their entirety and found in each case only a single base pair (bp) change in the 3' UTR (Fig. 1a, b). We then sequenced the 3' UTRs of the remaining seven *fem-3(gf)* mutants and found single-base pair changes in a 5-bp region in six of the alleles and a 112-bp deletion in the seventh and strongest allele (Fig. 1b, c). The finding of mutations in all nine *fem-3(gf)* 3' UTRs suggests this is the sole defect responsible for the *fem-3(gf)* phenotype. We propose that the switch from sperm to oocytes is regulated by the wild-type *fem-3* 3' UTR.

How does the 3' UTR regulate *fem-3* activity? One possibility is that it affects RNA levels. In *fem-3(gf)* mutants, *fem-3* might be activated by an increase in the synthesis or stability of *fem-3* RNA. To investigate this possibility, we compared wild-type and *fem-3(gf)* steady-state RNA levels (Fig. 2a, b). In the third and fourth larval stages (L3 and L4), the level of *fem-3* RNA in *fem-3(gf)* animals is similar or slightly less than that of wild

type (Fig. 2a, b), whereas in *fem-3(gf)* adults it is markedly decreased (Fig. 2b). The decrease seen in *fem-3(gf)* adults probably results from a lack of oocytes and not from the *gf* mutation itself: *fem-3* RNA levels are no longer reduced in a *fem-3(gf)* mutant making oocytes (*q20q77*, a *fem-3* gene carrying both *gf* and loss-of-function mutations in *cis*; ref. 1) (Fig. 2b). These results indicate that *fem-3(gf)* mutations probably do not act by increasing the steady-state levels of *fem-3* RNA and, further, that they are likely to act post-transcriptionally.

Comparison of *fem-3(+)* and *fem-3(gf)* RNAs also revealed an increase in the size and heterogeneity of *fem-3(gf)* RNAs in L4 and adult animals (Fig. 2c, and data not shown) that is not observed in mid-L3 to mid-L4 RNAs (Fig. 2a). To test whether this change was due to increased polyadenylation of *fem-3(gf)* RNAs, we compared RNAs with and without their poly(A) tails. In mid- to late-L4 animals, *fem-3(q96gf)* RNA migrates in a broader band than wild type (Fig. 2c, lanes 1 and 2), but when poly(A) tails are removed, the RNAs comigrate (Fig. 2c, lanes 3 and 4). Similar results were obtained for L4 and adult RNAs of both *fem-3(q20gf)* and *fem-3(q96gf)* (data not shown). We estimate that *fem-3(gf)* poly(A) tails range from 30 to 100 A residues, whereas *fem-3(+)* poly(A) tails are of ~30–50 residues (data not shown, see legend to Fig. 2). The developmental stages at which increased polyadenylation of *fem-3(gf)* RNA is observed coincide with the stages at which *fem-3(gf)* is inappropriately activated to make sperm.

One simple interpretation of the data is that *fem-3(gf)* mutations destroy a binding site for a negative regulator of *fem-3* RNA activity (Fig. 3a). Unable to bind the negative regulator, *fem-3(gf)* RNA would remain active and cause continuous

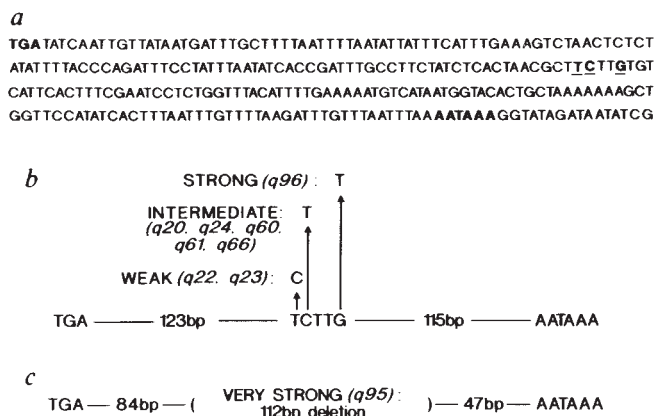


FIG. 1 Sequences of wild-type and mutant *fem-3* 3' UTRs: a, Wild-type *fem-3* 3' UTR sequence starting with base 1,402; numbering based on complementary DNA sequence and analysis of gene structure (T. Rosenquist, J.A. and J.K., manuscript in preparation). The translational stop and polyadenylation signal are in bold; nucleotides altered by *fem-3(gf)* point mutations are bold and underlined. No striking secondary structure (for example, stem-loop) is obvious near the mutations, and no sequences complementary to the *fem-3* 3' UTR are found in any other part of *fem-3*. b, *fem-3(gf)* point mutations. Mutants of equivalent strength¹ carry identical changes. c, *fem-3(q95gf)* deletion. The junction sequence created by the deletion (CTGCTGGT) is identical in 6 out of 8 positions to the wild-type region altered by *fem-3(gf)* point mutations (CTTCTTGT). Also, *fem-3(q95gf)* contains a G to A change at nucleotide 1,652, the G following the polyadenylation signal. METHODS. For each allele, a genomic library was made by cloning *Bgl*II-digested homozygous mutant DNA into the *Bam*HI site of λ EMBL3. Phage containing *fem-3* (as a 10 kb *Bgl*II fragment) was purified; a 5.5-kb *Sall*-*Bgl*III fragment containing the entire transcribed region of *fem-3* was subcloned from the λ phage into pIB176. Dideoxy chain termination sequencing was performed by standard methods using Sequenase (USB) and primers to *fem-3*. Both *q20gf* and *q22gf* were sequenced in the entire transcribed region plus 100 bp of flanking DNA; the other alleles were sequenced only in the 3' UTR.

* To whom correspondence should be addressed at the Laboratory of Molecular Biology, 1525 Linden Drive, Madison, Wisconsin 53706, USA.

spermatogenesis (Fig. 3b). If this hypothesis is true, exogenously expressed wild-type 3' UTR RNA would titrate this factor from endogenous *fem-3* RNA, whereas *fem-3(gf)* 3' UTR RNA should lack or have reduced titrating activity (Fig. 3c, d). Titration of a negative regulator is predicted to activate endogenous *fem-3* RNA inappropriately, leading to masculinization of the hermaphrodite germ line. To test this idea, we constructed plasmids designed to express either a wild-type (p-*wt*) or *fem-3(gf)* (p-*q95gf* or p-*q96gf*) 3' UTR. In each case, the *fem-3* 3' UTR and its 3' flanking region were placed downstream of the *fem-3* 5' flanking region and 50 nucleotides of the *fem-3* 5' UTR. The plasmids, which lacked the *fem-3* coding region, were introduced into wild-type animals (see legend to Fig. 4). As predicted, we found that p-*wt* masculinized the hermaphrodite germ line (Fig. 4e, f), but that p-*q95gf* or p-*q96gf* had little masculinizing activity (Fig. 4d, f). We interpret this result to mean that exogenous *fem-3(+)* 3' UTR, but not *fem-3(gf)* 3' UTR, competes with the endogenous wild-type *fem-3* 3' UTR for a negative regulator. The masculinizing activity is likely to be due to synthesis of 3' UTR RNA, because a plasmid containing only the wild-type 3' UTR plus 3' flanking DNA (p-*wt* 3' only) or one containing *fem-3* 5' flanking plus 5' UTR sequences

alone (p-*wt* 5' only) does not masculinize wild-type animals (Fig. 4f and legend to Fig. 4; T. Evans, personal communication).

Our working model is that late in L4 the wild-type *fem-3* 3' UTR binds a negative regulatory factor, which leads to shortening of the poly(A) tail and inactivation of *fem-3* RNA. Inhibition of *fem-3* would effect the switch to oogenesis (Fig. 3a). In other species, the lengthening of poly(A) tails on maternal RNAs can cause an increase in their translation⁴⁻⁷; we speculate that *fem-3(gf)* RNAs have escaped a negative translational control. The regulation could occur through a direct interaction with the translation or polyadenylation machinery, or be an indirect effect, for example, by localization of *fem-3* RNA to a compartment where it cannot be translated. There are precedents for the involvement of the 3' UTR in regulating translation⁴⁻¹⁰, and in the case of creatine kinase B regulation, soluble factor(s) have been shown to bind the 3' UTR *in vitro*¹¹.

How does negative regulation through the *fem-3* 3' UTR relate to the mechanism of sex determination in *C. elegans*? Gain-of-function mutations in *tra-2*, which interfere with a negative regulation required for the onset of hermaphrodite spermatogenesis^{12,13}, likewise fall in the 3' UTR of *tra-2* RNA (P. G. Okkema and J.K., manuscript in preparation). Because *fem-3(gf)* and *tra-2(gf)* mutations primarily affect the hermaphrodite germ line^{1,12,13}, this regulation probably does not operate in all tissues for the determination of sex in *C. elegans*. Instead, the proposed translational regulation of these genes through their 3' UTRs may control spermatogenesis in hermaphrodites. As *fem-3* is a maternal RNA (T. Rosenquist, J.A. and J.K., manuscript in preparation), we speculate that the regulation of *fem-3* by its 3' UTR may be related to a general mechanism of 'masking' maternal RNAs. Perhaps, in the evolution of hermaphroditism, transient spermatogenesis has been achieved by using an existing germ-line control of maternal messages. Masking

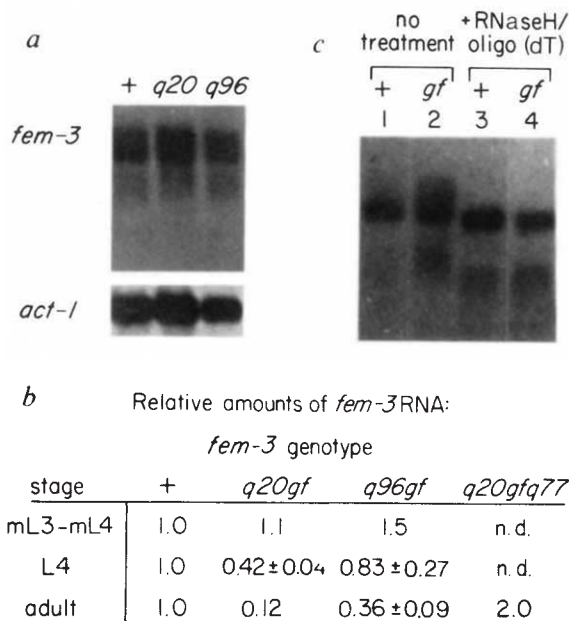


FIG. 2 Analysis of *fem-3(gf)* RNAs. **a**, Northern blot of mid-L3 to mid-L4 RNA prepared from *fem-3(+)*, *fem-3(q20gf)* and *fem-3(q96gf)* animals. Top panel, *fem-3* RNA; bottom panel, *act-1* RNA. **b**, Relative amounts of *fem-3* RNA in *fem-3(+)* and *fem-3* mutant animals. Numbers indicate the *fem-3* to *act-1* ratio, with wild type being set at 1.0. The variance shown for some entries gives the range of results from experiments done twice. L3, third larval stage; L4, fourth larval stage. **c**, Northern blot of wild-type (lanes 1 and 3) and *fem-3(q96gf)* (lanes 2 and 4) mid-late L4 RNAs before and after removal of poly(A) tails. Lanes 1 and 2, before treatment; lanes 3 and 4, RNAs treated with oligo(dT) and RNase H to remove poly(A) tails. **METHODS.** Embryos were isolated using hypochlorite treatment of gravid adults grown at 15 °C, the permissive temperature for *fem-3(gf)* (ref. 1), transferred to 25 °C, the restrictive temperature for *fem-3(gf)*, and incubated until they reached the desired stage. Both wild-type and *fem-3(gf)* strains carry the linked marker *dpy-20(e1282)*. For northern blots, 1–5 µg poly(A)⁺ RNA were used per lane; preparation of poly(A)⁺ RNA, formaldehyde-agarose gel electrophoresis, blotting and hybridization were as described³; *fem-3* and *act-1* were detected using ³²P-labelled RNAs made from pJK50, a partial *fem-3* cDNA in pIB176 and pT3/T7-18-103, an *act-1* specific clone (provided by M. Krause), respectively. Signals on northern blots were quantitated on a Betagen β scanner. RNase H digestion of poly(A) tails was essentially as described¹⁴. Poly(A) tail lengths were measured on northern blots by comparing the size of *fem-3* to markers of known size.

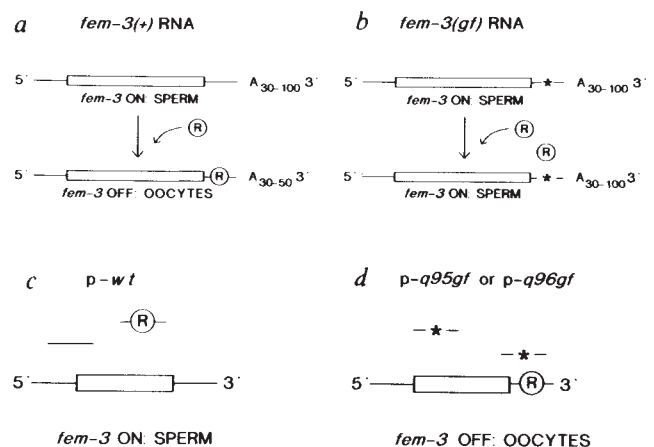


FIG. 3 Model for *fem-3* regulation and experimental design to test the model: *fem-3* RNA is represented by the open box (denoting coding region) with lines (5' and 3' UTRs); the star denotes a *fem-3(gf)* mutation. R, negative regulator. **a** and **b**, Model. In **a**, *fem-3* RNA is active when no regulator is bound to its 3' UTR and its poly(A) tail is relatively long; *fem-3* RNA is inactivated by binding a regulator to its 3' UTR and shortening its poly(A) tail. Active *fem-3* RNA directs spermatogenesis, whereas inactivation of *fem-3* RNA leads to the switch from spermatogenesis to oogenesis. In **b**, *fem-3(gf)* RNA is unable to bind the negative regulator; its poly(A) tail remains long and the RNA active resulting in continuous spermatogenesis. **c** and **d**, Test of the model. Construction of plasmids (p-*wt*, p-*q95gf* and p-*q96gf*) described in legend to Fig. 4. **c**, The exogenous expression of wild-type *fem-3* 3' UTR (solid lines) by p-*wt* is predicted to titrate R from endogenous *fem-3* RNA, causing inappropriate activity of *fem-3* and production of sperm instead of oocytes. **d**, The exogenous expression of a *fem-3(gf)* 3' UTR (line with star) by p-*q95gf* or p-*q96gf* is predicted not to titrate R from endogenous *fem-3* RNA, resulting in little or no effect on *fem-3* activity and production of oocytes in adults as usual.

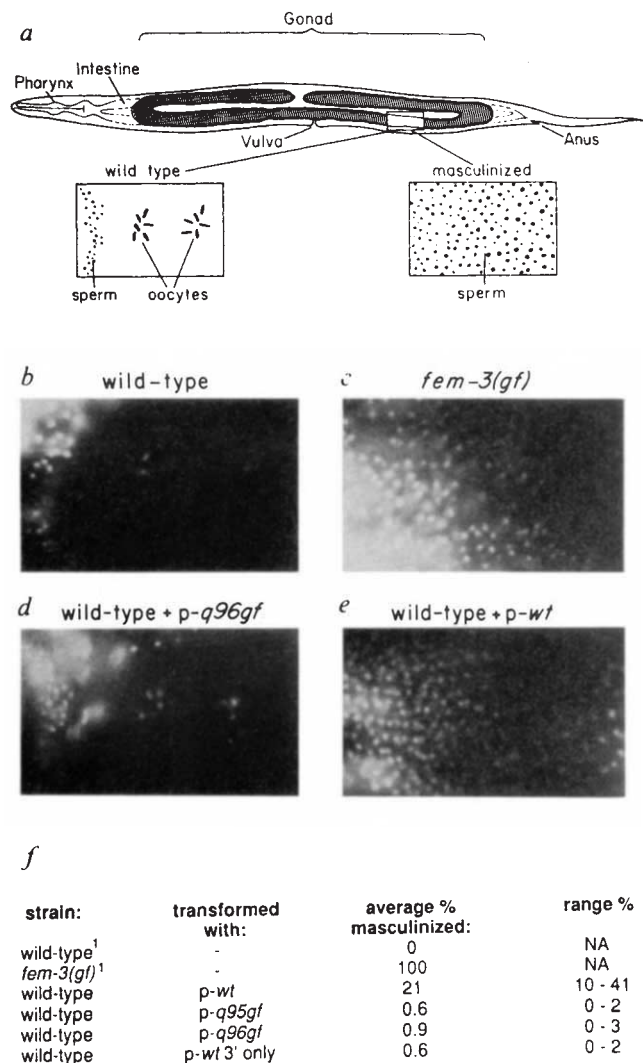


FIG. 4 Exogenous *fem-3(+)* 3' UTR masculinizes the germ line. *a*, Anatomy of a *C. elegans* adult hermaphrodite. Gonad is shaded; boxed region contains differentiated gametes and is enlarged to show a representation of DNA staining patterns from wild-type or masculinized germ lines. Dots represent condensed sperm nuclei; clusters of short bars represent oocyte chromosomes in meiotic diplotene. *b-e*, Photomicrographs of gametes from DAPI-stained worms. *b*, Untransformed wild-type (sperm plus two oocytes); *c*, untransformed *fem-3(q20gf)* (sperm only); *d*, wild-type transformed with p-*q96gf* (sperm plus two oocytes); *e*, wild-type transformed with p-wt (sperm only). *f*, Percentage of wild-type, *fem-3(gf)* and transformed animals with a masculinized germ line. The average percentage masculinization includes data from several independent lines. Number of lines and data: six p-wt lines (10%, 11%, 21%, 21%, 25%, 41%); three p-*q95gf* lines (0%, 0%, 2%); three p-*q96gf* lines (0%, 0%, 3%); three p-wt 3' only lines (0%, 0%, 1%). METHODS. Plasmids were constructed using a plasmid carrying 1.2 kb of 5' flanking region and 50 bp of 5' UTR from *fem-3* (p-wt 5' only, pJK228; T. Evans, personal communication); the backbone is pPD16.43 (ref. 15). After removal of the *lacZ* sequence, a *Clal-HindIII* fragment carrying the entire 3' UTR plus 755 bp of 3' flanking region from *fem-3(+)*, *fem-3(q95gf)* or *fem-3(q96gf)* was inserted to make p-wt (pJK275), p-*q95gf* (pJK277) or p-*q96gf* (pJK276), respectively; p-wt 3' only (pJK222) is this wild-type *Clal-HindIII* fragment inserted into pPD16.43. Transformation was as described¹⁶, except that injection was into distal gonadal arms. Wild-type animals were coinjected with 100 $\mu\text{g ml}^{-1}$ of the plasmid of interest plus 100 $\mu\text{g ml}^{-1}$ pRF4, which contains a dominant *rol-6* gene. pRF4 incorporated into extrachromosomal arrays causes animals to roll (C. Mello, J. Kramer, V. Ambros and D. Stinchcomb, personal communication). Rollers contained from 10 to 50 copies of *fem-3* DNA of the appropriate size as determined by Southern blot quantitation, normalizing for the percentage of rollers (data not shown). For determination of percentage masculinization, L2 to L3 rollers were picked, grown to adulthood (2 days at 25 °C), and examined by Nomarski microscopy. An animal was counted as masculinized if at least one gonad arm contained only sperm. From 50 to 150 rollers were scored for each line. Of three p-wt 5' only lines, one was examined by Nomarski microscopy; 0/50 animals were masculinized. The other two lines were examined in the dissecting microscope. Hermaphrodites with a masculinized germline produce neither oocytes nor eggs which is a distinctive phenotype; no such animals were detected (T. Evans, personal communication). For DAPI staining, rollers were washed in distilled H₂O, incubated in methanol or ethanol containing 200 ng ml⁻¹ DAPI for 20 min, washed once in distilled H₂O and mounted on agarose pads for observation and photography (E. Lambie, personal communication).

machinery might become activated during hermaphrodite spermatogenesis and turn off *fem-3*, effecting the switch to oogenesis. Consistent with this idea is the discovery of *mog-1*, a candidate negative regulator of *fem-3*, which is also maternally required for embryogenesis (P. Graham and J.K., unpublished). Perhaps *mog-1* is involved in masking *fem-3* and other maternal messages; the masking of *fem-3* could turn *fem-3* off, resulting in the switch from spermatogenesis to oogenesis. □

MAP2 kinase and 70K S6 kinase lie on distinct signalling pathways

Lisa M. Ballou*, Heide Luther & George Thomas†

Friedrich Miescher-Institut, Postfach 2543, CH-4002 Basel, Switzerland

ACTIVATION of protein synthesis is required for quiescent cells to transit the cell cycle¹, and seems to be mediated in part by phosphorylation of the 40S ribosomal protein, S6 (ref. 2). A mitogen-activated S6 kinase of relative molecular mass 70,000 (70K) has been isolated from mouse fibroblasts^{3,4} as well as from avian, rat and rabbit tissues⁵⁻⁹. Comparison of complementary DNA sequences shows that this enzyme¹⁰ is distinct from S6 kinase II (92K)¹¹ found in *Xenopus* eggs¹² and fibroblasts^{13,14}. Both kinases are activated by serine/threonine phosphorylation^{3,15-18}, suggesting that at least one serine/threonine kinase links receptor tyrosine kinases with S6 kinases. A candidate for this link is MAP2 kinase, which is rapidly activated by tyrosine/threonine phosphorylation following mitogenic stimulation¹⁹⁻²³. Incubation of MAP2 kinase from insulin-treated 3T3-L1 adipocytes with phosphatase-inactivated S6 kinase II from *Xenopus* leads to partial reactivation and phosphorylation of the enzyme¹⁷. These and other findings⁸ have led to the suggestion that MAP2 kinase also activates the

* Present address: Institute for Molecular Pathology, Dr. Bohr-Gasse 7, A-1030 Vienna, Austria.
† To whom correspondence should be addressed.

Received 18 September; accepted 19 November 1990.

- Barton, M. K., Schedl, T. & Kimble, J. *Genetics* **115**, 107-119 (1987).
- Hodgkin, J. *Genetics* **114**, 15-52 (1986).
- Rosenquist, T. A. & Kimble, J. *Genes Dev.* **2**, 606-616 (1988).
- Wickens, M. *Trends biochem. Sci.* **15**, 320-324 (1990).
- Jackson, R. J. & Standart, N. *Cell* **62**, 15-24 (1990).
- McGrew, L. L., Dworkin-Rastl, E., Dworkin, M. B. & Richter, J. D. *Genes Dev.* **3**, 803-815 (1989).
- Vassalli, J.-D. *et al. Genes Dev.* **3**, 2163-2171 (1989).
- Braun, R. E., Peschon, J. J., Behringer, R. R., Brinster, R. L. & Palmiter, R. D. *Genes Dev.* **3**, 793-802 (1989).
- Kruys, V. *et al. Proc. natn. Acad. Sci. U.S.A.* **84**, 6030-6034 (1987).
- Kruys, V., Marinx, O., Shaw, G., Deschamps, J. & Huez, G. *Science* **245**, 852-854 (1989).
- Ch'ng, J. L. C., Shoemaker, D. L., Schimmel, P. & Holmes, E. W. *Science* **248**, 1003-1006 (1990).
- Doniach, T. *Genetics* **114**, 53-76 (1986).
- Schedl, T. & Kimble, J. *Genetics* **119**, 43-61 (1988).
- Vournakis, J. N., Efstratiadis, A. & Kafatos, F. C. *Proc. natn. Acad. Sci. U.S.A.* **72**, 2959-2963 (1977).
- Fire, A., Harrison, S. M. W. & Dixon, D. *Gene* **93**, 189 (1990).
- Fire, A. *EMBO J.* **5**, 2673-2680 (1986).

ACKNOWLEDGEMENTS. We are grateful to T. Evans and M. Wickens for discussions; T. Evans, E. B. Goodwin, P. Kuwabara and M. Wickens for comments on the manuscript; A. Fire for pPD16.43; C. Mello for pRF4; and L. Olds for technical assistance. This work was supported by the NSF (J.A.), and by the NIH (J.A. and J.K.).